

Evidence for C–H···O=C Bonding in Coadsorbed Aromatic–Carbonyl Systems on Pt(111)

Stéphane Lavoie and Peter H. McBreen*

Département de Chimie, Université Laval, Québec (QC), Canada G1K 7P4

Received: March 9, 2005; In Final Form: April 27, 2005

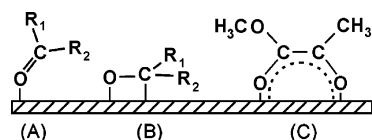
The coadsorption of ethyl formate, acetone, and methyl pyruvate with benzene and naphthalene on Pt(111) was studied with reflection absorption infrared spectroscopy (RAIRS) and thermal desorption (TPD) measurements. Coadsorbed benzene or naphthalene are found to convert η^1 - and η^2 -states of ethyl formate and acetone into new states displaying slightly red-shifted carbonyl bands. Similarly, coadsorption converts the enediolate state of methyl pyruvate into a new adsorption geometry in which the carbonyl bands are silent. In each case, coadsorption of the aromatic leads to significantly modified carbonyl desorption spectra. The results suggest an attractive carbonyl–aromatic interaction that weakens or removes the direct interaction of the carbonyl function with the metal surface. The aromatic–carbonyl interaction is attributed to hydrogen bonding between C–H and C=O, enhanced by the chemisorption induced polarization of the aromatic.

Introduction

Ordered molecular monolayers on metal single-crystal surfaces are the result of several intermolecular and molecule–metal interactions. The adsorbate–adsorbate interactions include both through-metal and metal-moderated through-space contributions.¹ Interactions which are only weakly present in the gas phase may be significantly enhanced in the chemisorbed state. A case in point is the report by Gao et al.² of a hydrogen-bonding interaction between coadsorbed ethylene and molecular oxygen on Ag(110). This interaction, observed in STM experiments at 13 K, is attributed to enhanced electrostatic interaction due to charge transfer from the metal to O₂.² On the basis of DFT calculations, Gao et al. estimated the H-bond strength to be at least 8.5 kJ/mol. Similarly, Jenkins and King³ reported that coadsorption of potassium and carbon monoxide on Co(1010) gives rise to a greatly enhanced polarization of adsorbed CO, leading to a highly unusual structure with the K atom situated slightly higher than the level of the oxygen atom. Several studies have shown that coadsorption of CO⁴ or NO⁵ drives the formation of ordered benzene structures on metal surfaces. Somorjai et al.^{4a,b} attributed the formation of ordered CO/benzene structures on Rh(111) to an indirect interaction caused by the opposing net charge transfer in the coadsorbates. Thus, benzene adsorbs in the electron-deficient region created by back-donation into the CO $2\pi^*$ orbital, in a manner similar to the observed decoration by benzene of electron-deficient upper step edges of Cu(111).⁶ Stichler et al.⁵ proposed an additional unspecified direct, orbital overlap, interaction between NO and benzene on Rh(111). In particular, they noted that coadsorption leads to an increase in the adsorption energy as well as in the metal–molecule distance for benzene. A recent DFT study of CO/benzene on Ni(111) shows that self-organization in this case is driven to a roughly equal extent by benzene–benzene repulsion and benzene–CO attraction.⁷ The latter investigation also revealed that the attractive interaction for the $(2\sqrt{3} \times 2\sqrt{3})R30^\circ$ C₆H₆/2CO system leads to an increased net adsorption energy, and also to a pronounced reduction of electron density at the oxygen atom of CO.

The present paper deals with the coadsorption of benzene or naphthalene with three carbonyl compounds: ethyl formate, acetone, and methyl pyruvate. These systems differ from the CO or NO/benzene coadsorption systems in a number of respects. First, CO on noble metal surfaces is always adsorbed in a nearly vertical configuration with the oxygen atom pointing away from the surface, regardless of the adsorption site.⁸ In contrast, both η^1 and η^2 adsorption states are found for carbonyl molecules on metal surfaces (Chart 1). The bonding interaction is radically different for η^1 and η^2 chemisorption. The former involves the interaction of an oxygen lone-pair with the metal. In contrast, η^2 chemisorption results in extensive rehybridization of the carbonyl bond leading to single bond character.^{9–11} In addition, there is experimental evidence for the formation of π -adsorbed states, where the weakly perturbed carbonyl bond lies parallel to the surface.¹¹ Hence, at least three molecular states, displaying significantly different adsorption geometries, are energetically accessible for carbonyl compounds on noble metal surfaces. Second, the differential heats of adsorption of CO and benzene on Pt(111) are very close, with initial heats of adsorption of 180 and 197 kJ/mol, respectively.^{12,13} The benzene adsorption energy is, however, due to the interaction of six carbon atoms with the surface. Furthermore, as pointed out by Yamagishi et al.,⁷ only small energy barriers separate different flat-lying configurations of chemisorbed benzene. Thus, CO is likely to direct benzene into new adsorption sites. In contrast, the heat of adsorption of benzene on Pt(111) is significantly larger than that for acetone on the same surface.^{11,14} Vannice et al. estimated adsorption energies of 52 and 48 kJ/mol for η^2 - and η^1 -acetone, respectively, on Pt(111).¹¹ Hence, intuitively, benzene might be expected to direct the adsorption of coadsorbed carbonyls into specific surface sites. This study probes the influence of adsorbed benzene on the adsorption configurations of coadsorbed carbonyl molecules. As pointed out below, the coadsorption of aromatic and carbonyl molecules on Pt(111) is of particular interest in the context of the Orito reaction.¹⁵ The Orito reaction describes the enantioselective hydrogenation of α -ketoesters on chiral-modified Pt surfaces. Acetone, ethyl formate, and methyl pyruvate are respectively keto-carbonyl, ester-carbonyl, and α -ketoester molecules.

* Address correspondence to this author. E-mail: peter.mcBreen@chm.ulaval.ca.

CHART 1: Carbonyl Adsorption Geometries^a

^a A: η^1 . B: η^2 . C: enediolate.

Experimental Section

The experiments were performed in an ultrahigh vacuum system equipped for reflection absorption infrared spectroscopy (RAIRS), Auger electron spectroscopy (AES), and temperature programmed desorption (TPD) measurements. The base pressure of the chamber was 8×10^{-11} Torr. The Pt(111) sample was cleaned by repeated Ar⁺ sputtering, treatment in 2×10^{-7} Torr of O₂ at 900 K, and annealing to 1100 K. Surface cleanliness was verified by AES, and by TPD and RAIRS tests with CO. Acetone, ethyl formate, and methyl pyruvate purchased from Sigma-Aldrich were further purified by freeze-thaw cycles in the gas-handling line. Exposure to adsorbates was achieved by backfilling the chamber to 6.0×10^{-10} Torr. All RAIRS spectra were recorded with the sample at 110 K. Up to six *m/e* peaks were monitored in each thermal desorption ramp to correctly identify each desorption peak.

Results

RAIRS data for chemisorbed methyl pyruvate, acetone, ethyl formate, and the corresponding coadsorption with benzene are displayed in Figure 1. Chemisorbed benzene did not show any RAIRS bands in the 1000–3200 cm⁻¹ range in agreement with literature data.¹⁶ Multilayer growth begins at exposures above 0.3 L as detected by a molecular desorption peak at 170–180 K. Coadsorption experiments with coverages of benzene close to 0.3 ML were performed by first annealing the benzene layer from 110 to 200 K and then cooling to 110 K.

Ethyl formate forms an η^1 -chemisorbed monolayer characterized by oppositely shifted $\nu(\text{C=O})$ and $\nu(\text{C-O}_e)$ bands at 1613 and 1276 cm⁻¹ (spectrum 1a). The corresponding bands for amorphous ethyl formate are observed at 1723 and 1193 cm⁻¹, respectively.¹⁷ They are observed at 1648–1665 and 1232–1259 cm⁻¹ for η^1 -chemisorbed ethyl formate on Ni(111).¹⁸ Annealing from 110 to 170 K results in spectrum 1b, in which the carbonyl and ester bands are absent. Spectrum 1b is consistent with an adsorption state where the carbonyl function is η^2 -(C,O) bonded to the surface with the OCH₂CH₃ function oriented roughly parallel to the surface. The bands at 1438 and 1160 cm⁻¹, in spectrum 1b, may be attributed to $\delta_{\text{as}}(\text{CH}_3)$ and out-of-plane OCH₂CH₃ rocking vibrations.^{17,18} Exposure of η^1 - and η^2 -states to benzene yields spectrum 1c, displaying carbonyl, methyl deformation, and ester bands at 1709, 1438, and 1190 cm⁻¹, respectively. These bands are present in greater intensity in experiments performed by first exposing to benzene and then to ethyl formate, spectrum 1d. The latter spectrum also displays a condensed layer carbonyl band, at 1724 cm⁻¹. The disappearance of the η^1 -state carbonyl band at 1613 cm⁻¹ and the appearance of a slightly red-shifted carbonyl band at 1709 cm⁻¹ in its place is consistent with an adsorbed state in which the carbonyl-surface interaction is very weak. In this context, we note that η^1 -adsorption of acetone on Au(111), a very inert surface, leads to a red-shift of more than 30 cm⁻¹ in the carbonyl band.¹⁹ Hence, the 15 cm⁻¹ red-shift observed for ethyl formate coadsorbed with benzene (spectrum 1d) suggests that the carbonyl function is not in contact with the Pt(111) surface.

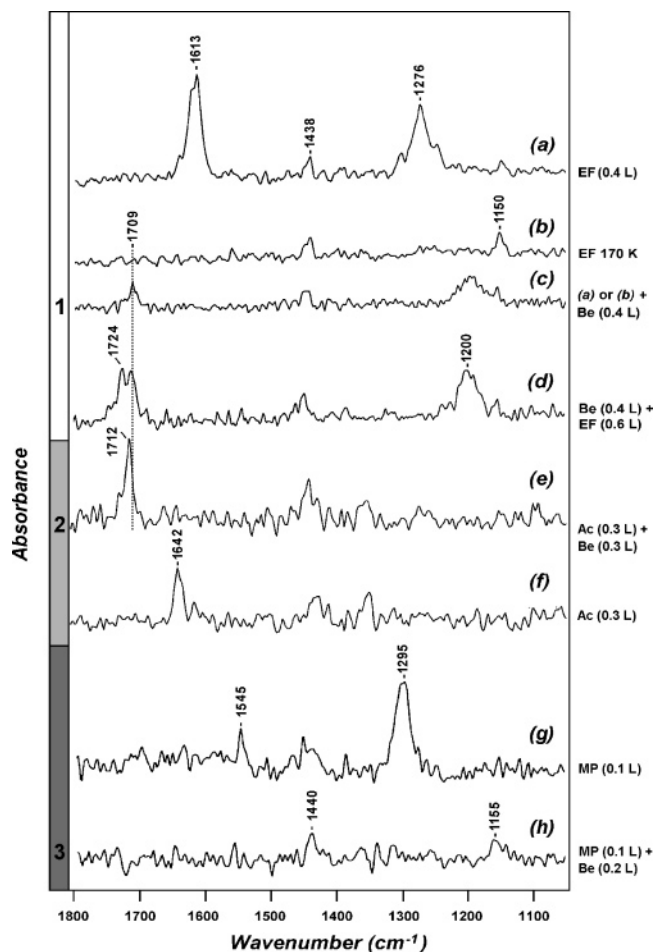


Figure 1. RAIRS spectra for ethyl formate (EF), acetone (Ac), and methyl pyruvate (MP) on clean Pt(111) at 110 K, and for EF, Ac, and MP coadsorbed with benzene (Be). Multilayer growth for benzene, EF, Ac, and MP begins at exposures of 0.3, 0.6, 0.5, and 0.45 L, respectively. (1 L = 1×10^{-6} Torr·s.)

The changes induced by coadsorption as observed in the RAIRS measurements are also clearly reflected in the thermal desorption data shown in Figure 2. Ethyl formate on clean Pt(111) displays molecular desorption peaks at 140, 155, and 190 K (spectrum 2a) and a decarbonylation peak at 415 K. Several *m/e* peaks were monitored to differentiate ethyl pyruvate and CO desorption. The peak at 140 K arises from desorption from the multilayer. The RAIRS data indicate that the peak at 155 K is associated with the transition from η^1 - to η^2 -bonding. The peak at 190 K is due to molecular desorption in competition with decarbonylation of the η^2 -state. At low coverages (spectrum 2b), only the molecular peak at 190 K and the CO peak at 415 K are observed. In contrast, coadsorption with benzene leads to an intense molecular desorption peak at 160 K and a weak decarbonylation peak (spectrum 2c). Evidently, coadsorption of benzene inhibits the formation of the η^2 -state and hence the decarbonylation reaction. The new desorption peak at 160 K is observed for benzene exposures less than 0.02 L. The peak at 190 K is completely removed by exposure to 0.25 L benzene.

Results for RAIRS experiments on acetone and acetone/benzene coadsorption are shown as spectra 1f and 1e, respectively. The carbonyl band at 1642 cm⁻¹ in spectrum 1e is characteristic of an η^1 -state. A number of studies have shown that acetone undergoes η^1 -chemisorption on defect-free Pt(111) at 100 K, and that chemisorption at defect sites leads to a minority η^2 -state.^{10,11} The present study, confirming the results of Vannice et al., shows that η^1 -acetone on Pt(111) can be

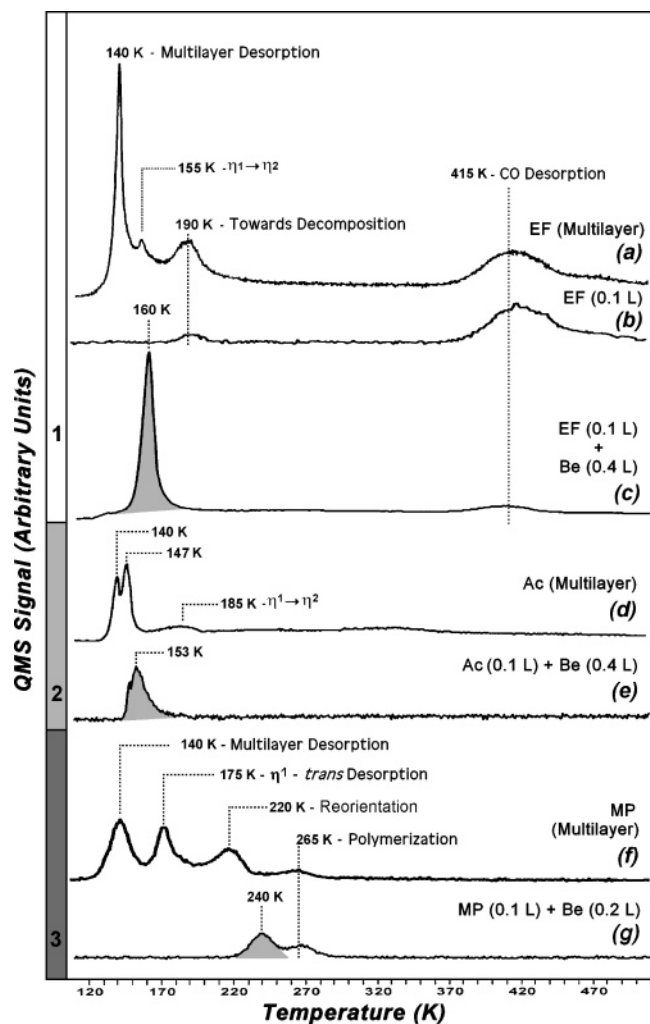


Figure 2. TPD spectra (m/e 28) for ethyl formate (EF), methyl pyruvate (MP), and acetone (Ac) on clean Pt(111) (a, b, d, and f). Spectra for coadsorbed benzene (Be) and EF, Ac, and MP on Pt(111) (c, e, and g).

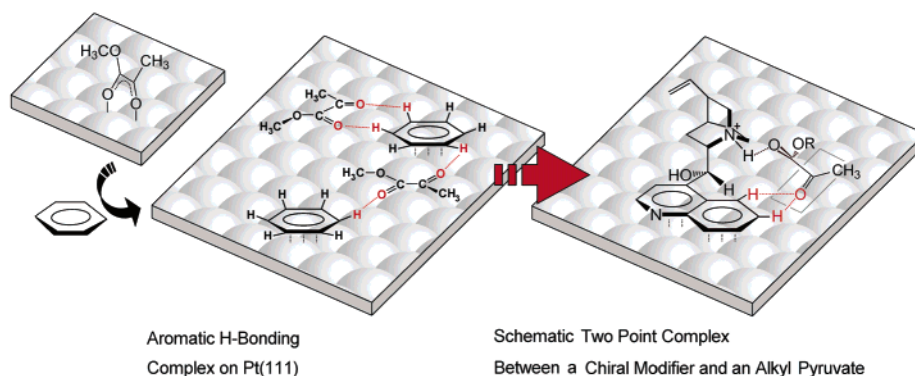
converted to an η^2 -state by annealing to 185–200 K.¹¹ Vannice et al. also found that the η^1 -state disappears as the coverage is increased toward the full monolayer. They attributed this high-coverage state, displaying a carbonyl stretching frequency of $\sim 1700\text{ cm}^{-1}$, to either the formation of a second layer prior to completion of the monolayer or the formation of a π -adsorbed state.¹¹ The carbonyl band for multilayer acetone on Pt(111) is observed at 1719 cm^{-1} . Spectrum 1e shows that coadsorption with benzene at 110 K also removes the η^1 -state, replacing the carbonyl band at 1642 cm^{-1} with a new one at 1712 cm^{-1} . The thermal desorption measurements reflect the coadsorption induced changes seen in the RAIRS data. Multilayer acetone desorbs from clean Pt(111) at 144 K, and molecular desorption at 185 K competes with conversion from η^1 - to η^2 -adsorbed states (spectrum 2d). Coadsorption with benzene, however, leads to a single desorption peak at 153 K (spectrum 2e).

RAIRS spectra for methyl pyruvate and methyl pyruvate/benzene on Pt(111) are shown as spectra 1g and 1h, respectively. The adsorption of methyl pyruvate at 110 K forms an enediolate state characterized by a band at 1545 cm^{-1} (spectrum 1g).²⁰ The intense band at 1295 cm^{-1} is attributed to the $\nu(\text{C}-\text{O}_\text{e})$ (ester) stretching vibration.²⁰ Coadsorption with benzene removes the enediolate state leaving two weak bands at 1440 and 1155 cm^{-1} (spectrum 1h). The absence of intensity due to the carbonyl and $\nu(\text{C}-\text{O}_\text{e})$ bands and the presence of the OCH_3

out-of-plane rocking band²¹ at 1155 cm^{-1} are consistent with an adsorption geometry in which the molecular plane is parallel to the surface. Hence, as in the case of acetone and ethyl formate, coadsorption with benzene drives methyl pyruvate into a new adsorption state. And, as with the other two carbonyls, the modification is clearly reflected in thermal desorption measurements. Methyl pyruvate on Pt(111) displays four molecular desorption peaks (spectrum 2f).²² The peaks at 140 and 175 K are due, respectively, to desorption from the multilayer and the high-coverage η^1 -state. The peak at 220 K coincides with the conversion of the enediolate into a new, flat-lying, state.²² The peak at 265 K coincides with CH bond scission and the onset of the polymerization reaction reported by Bonello et al.²³ Coadsorption with benzene results in molecular desorption peaks at 240 and 265 K (spectrum 2g), consistent with the inhibition of the enediolate and the formation of a new chemisorbed state. The polymerization reaction, however, is not totally suppressed. Presumably polymerization requires a flat-lying precursor, and as discussed above, coadsorption with benzene results in such a flat-lying state. Additional measurements were made on the coadsorption of the carbonyl molecules with naphthalene and cyclohexane. Experiments performed with naphthalene show similar coadsorption effects to those presented above for benzene. In contrast, experiments performed with cyclohexane coadsorption show simply an additive behavior yielding no evident perturbation of the chemisorbed carbonyls.

Discussion

Benzene coadsorption is found to limit the number of adsorption states for ethyl formate, acetone, and methyl pyruvate on Pt(111). The RAIRS data show that coadsorbed benzene converts the η^1 - and η^2 -states of ethyl formate and the η^1 -state for acetone into new states displaying only slightly red-shifted carbonyl bands. Coadsorption also converts the enediolate state of methyl pyruvate into a new state in which the carbonyl bands are silent. These results thus suggest a specific interaction between carbonyls and coadsorbed aromatics leading to a weakly adsorbed carbonyl state. Weakly adsorbed states are a common characteristic of high coverages, where the packing density leads to interadsorbate repulsion and the occupation of higher energy surface sites. However, the coadsorption phenomena observed in this study are not due to high coverage effects. This was verified by performing experiments with a range of submonolayer coverages of benzene. Even coverages below 0.1 of a monolayer were found to convert coadsorbed carbonyls. Thus, the results indicate that benzene cooperates with the substrate to trap carbonyl molecules. This cooperation is reflected in the thermal desorption data. Desorption from the η^1 -states of ethyl formate and acetone occurs at 155 and 185 K, respectively. This is consistent with weaker chemisorption of ester-carbonyls as compared to keto-carbonyls.²⁴ However, on coadsorption with benzene, acetone and ethyl formate desorb in the inverse order, at 153 and 160 K, respectively. This result suggests that the adsorption energy for acetone or ethyl formate coadsorbed with benzene is not determined by the metal-carbonyl interaction. This, in turn, indicates that the carbonyl bond is not preferentially directed toward the surface. To account for the observed data, we propose that the attractive potentials between acetone, ethyl formate, methyl pyruvate, and coadsorbed benzene contain a direct component. In particular, we propose a role for a $\text{C}-\text{H}\cdots\text{O}=\text{C}$ hydrogen bonding interaction. The RAIRS data for the ethyl formate/benzene coadsorption system displays an $\Delta\nu = 15\text{ cm}^{-1}$ red-shift (spectrum 1d) of

CHART 2: Relevance to the Orito Reaction of C–H···O=C Bonding in Coadsorbed Aromatic–Carbonyl Systems

the carbonyl band. A weaker red-shift, 7 cm^{-1} , is observed for coadsorbed acetone and benzene. The carbonyl bands are silent for methyl pyruvate coadsorbed with benzene, hence there is no information on a possible shift in $\nu(\text{CO})$ frequency. The observed frequency changes for ethyl formate and acetone are close to the 16 and 9 cm^{-1} red-shifts attributed to C–H···O=C bonding in liquid cyclopentanone and cyclohexanone, respectively.²⁵ As mentioned above, chemisorbed benzene does not display RAIRS intensity in the $\nu(\text{CH})$ stretching region. Hence, the fact that an enhanced $\nu(\text{CH})$ signal for coadsorbed benzene was not observed in this study may not be used to rule out a hydrogen bonding interaction.

The phenomenon of hydrogen bonding to aromatics is now established in the literature. More precisely, there are a number of examples dealing with activated aromatic systems. In-plane H-bonding has been observed in benzene cation/ H_2O or CH_3OH charge-dipole clusters with use of IR spectroscopy.²⁶ Similarly, a C–H···O=C type interaction between dianionic *p*-benzoquinone and a benzene hydrogen is indicated by simulations performed by Manojkumar et al.²⁷ Recently, Venkatesan et al. used fluorescence-detected IR to observe C–H···O bonding in H_2O –1,2,4,5-tetrafluorobenzene jet-cooled clusters.²⁸ We propose that C–H···O=C bonding is observed in the coadsorbed systems as a result of the activation of the aromatic through its chemisorption interaction with the metal surface. Chemisorbed benzene behaves as a nucleophile and electron density is redistributed toward metal orbitals.²⁹ Density functional (DFT) calculations^{29a} show that adsorption of benzene on the energetically favorable bridge site on Pt(111) leads to a tilting of the H atoms away from the surface, a depopulation of electron density in all of the CH bonds, and a relaxation of the underlying surface. Low-temperature STM images of benzene on the 3-fold hollow site on Pt(111) show a modification of the local density of states 6–10 Å away from the center of the adsorbed molecule.⁶ We propose that polarization of the adsorbed aromatic combined with the local modification of the metal leads to the destabilization of the intrinsic adsorption states for all three carbonyls studied, and also leads to $\text{C}^\alpha\text{--H}\cdots\text{O}=\text{C}$ bond formation. Here, the suffix α emphasizes the aromatic-to-metal charge transfer. The proposed origin of the interaction is thus similar to that given by Gao et al. for H-bonding between O_2 and C_2H_4 on Ag(110).² From another perspective, the chemisorption interaction activates benzene in an analogous fashion to the fluorine atoms in 1,2,4,5-tetrafluorobenzene.²⁸ The observation of carbonyl bands for both acetone and ethyl formate is attributed to the crown-like²⁹ structure of chemisorbed benzene with the H atoms tilted away from the surface.

Adsorbate–adsorbate interactions in coadsorbed systems are of general interest due to the role that they can play in self-assembly for nanotechnological applications.^{1d} However, the

systems investigated in this study are of specific interest in relation to chiral catalysis at surfaces, and in particular to the Orito reaction.^{31,32} All effective modifiers for the Orito reaction contain an extended aromatic function by which the modifier is anchored to the platinum surface.³³ Hence, all known modifier–substrate pairs for this reaction are effectively aromatic–carbonyl coadsorption systems. In addition to an aromatic anchor, all known modifiers for the Orito reaction contain a function capable of conventional hydrogen bonding. In a previous study on Pt(111),²⁰ we reported RAIRS evidence for a conventional hydrogen bond between the ester group of methyl pyruvate and the amine group of naphthylethylamine, an effective modifier for Orito reactions.³⁴ The possibility of a second hydrogen-bonding interaction involving the keto-carbonyl of methyl pyruvate and the aromatic group of naphthylethylamine was also raised in previous publications.^{20,30} The present results show, indeed, that aromatic–carbonyl interactions on Pt(111) lead to marked changes in adsorption geometry, and also to significant changes in the stability of adsorbed carbonyls. The changes in adsorption geometry are attributed to a previously unrecognized direct interaction in the form of aromatic–carbonyl C–H···O=C bonding arising from the electrophilic interaction of the metal with the aromatic. The resulting C–H···O=C interaction is thus analogous to the Lewis acid enhanced Brønsted acid effect exploited by Yamamoto et al. for the design of homogeneous asymmetric catalysts.³⁵ The existence of such an interaction implies two-point attractive contact between coadsorbed dicarbonyls and chiral modifiers containing an aromatic anchor as well as an accessible center capable of conventional hydrogen bonding. In combination with the nonaromatic part of the modifier the second attractive interaction serves to orient and lock the α -ketoester into a two-point docking complex. Bidentate chelation is a widespread characteristic of homogeneous asymmetric catalysis³⁶ and it is now increasingly recognized that hydrogen bonding can lead to asymmetric induction in homogeneous chemistry.³⁷ Chart 2 is a schematic illustration of how two distinct hydrogen bonds between methyl pyruvate and cinchonidine, a chiral modifier, on Pt would lead to energetically different faces of the prochiral ketoester. Baiker et al. convincingly pointed out that the aromatic anchor can serve a steric role in the Orito reaction.³⁸ They proposed that this repulsive interaction between the ester moiety of the α -ketoester coupled with conventional H-bonding of the keto-carbonyl to the modifier induces asymmetric hydrogenation. As illustrated in Chart 2, we are proposing that the interaction with the aromatic anchor is attractive and that it involves H-bonding to the keto-carbonyl. It should be noted that the orientation of the keto-moiety in Chart 2 also avoids a possible repulsive interaction of the methyl group with the aromatic anchor.

Conclusions

RAIRS and TPD studies of acetone, ethyl formate, or methyl pyruvate coadsorbed with benzene or naphthalene on Pt(111) reveal a strong aromatic–carbonyl interaction. This interaction leads to the depopulation of the adsorption states preferred on the clean surface. In the case of methyl pyruvate, the enediolate state characteristic of clean Pt(111) is replaced by a flat-lying state in which the carbonyl bands are infrared silent. The geometry changes induced by coadsorption were considered within the context of literature data for benzene chemisorption, benzene–coadsorbate interactions, metal-moderated interadsorbate interactions, and recent reports on weak hydrogen-bonding interactions. It is proposed that the observed aromatic–carbonyl interaction is a result of chemisorption induced polarization of benzene leading to H-bond formation. The proposed interaction is thus analogous to the Lewis-acid enhanced Bronsted acid chemistry developed by Yamamoto et al.³⁵ The observed aromatic–carbonyl interaction needs to be considered in discussions of the Orito reaction, since all known modifier–substrate pairs effectively include an aromatic–carbonyl coadsorption component.

Acknowledgment. This work was supported by NSERC and FQRNT research grants and scholarships (S.L.).

References and Notes

- (1) (a) Humblot, V.; Barlow, S. M.; Raval, R. *Prog. Surf. Sci.* **2004**, 76, 1. (b) Barlow, S. M.; Raval, R. *Surf. Sci. Rep.* **2003**, 50, 201. (c) Feibleman, P. J. *Annu. Rev. Phys. Chem.* **1989**, 40, 261. (d) Merrick, M. L.; Luo, W.; Fichtorn, K. A. *Prog. Surf. Sci.* **2003**, 72, 117. (e) Scudiero, L.; Hipps, K. W.; Barlow, D. E. *J. Phys. Chem. B* **2003**, 107, 2903. (f) Hyldgaard, P.; Einstein, T. L. *Surf. Sci.* **2003**, 532, 600.
- (2) Gao, S. W.; Hahn, J. R.; Ho, W. *J. Chem. Phys.* **2003**, 119, 6232.
- (3) Jenkins, S. J.; King, D. A. *J. Am. Chem. Soc.* **2000**, 122, 10610.
- (4) (a) Barbieri, A.; Van Hove, M. A.; Somorjai, G. A. *Surf. Sci.* **1994**, 306, 261. (b) Yoon, H. A.; Salmeron, M.; Somorjai, G. A. *Surf. Sci.* **1997**, 373, 300. (c) Chiang, S. *Chem. Rev.* **1997**, 97, 1083.
- (5) Stichler, M.; Weimer, R.; Menzel, D. *Surf. Sci.* **1997**, 384, 179.
- (6) Sykes, E. C. H.; Han, P.; Kandel, S. A.; Kelly, K. F.; McCarty, G. S.; Weiss, P. S. *Acc. Chem. Res.* **2003**, 36, 945.
- (7) Yamagishi, S.; Jenkins, S. J.; King, D. A. *J. Am. Chem. Soc.* **2004**, 126, 10962.
- (8) Nowicki, M.; Emundts, A.; Pirug, G.; Bonzel, H. P. *Surf. Sci.* **2001**, 478, 180.
- (9) (a) Anton, A. B.; Avery, N. R.; Toby, B. H.; Weinberg, W. H. *J. Am. Chem. Soc.* **1986**, 108, 684. (b) Mavrikakis, M.; Barteau, M. A. *J. Mol. Catal. A: Chem.* **1998**, 131, 135.
- (10) Avery, N. R. *Surf. Sci.* **1983**, 125, 771.
- (11) (a) Vannice, M. A.; Erley, W.; Ibach, H. *Surf. Sci.* **1991**, 254, 1. (b) Liu, Z. M.; Vannice, M. A. *Surf. Sci.* **1994**, 316, 337.
- (12) (a) Yeo, Y. Y.; Vattuone, L.; King, D. A. *J. Chem. Phys.* **1997**, 106, 392. (b) Brown, W. A.; Kose, R.; King, D. A. *Chem. Rev.* **1998**, 98, 797.
- (13) Ihm, H.; Ajo, H. M.; Gottfried, J. M.; Bera, G. P.; Campbell, C. T. *J. Phys. Chem. B* **2004**, 108, 14627.
- (14) Alcala, R.; Greeley, J.; Mavrikakis, M.; Dumesic, J. A. *J. Chem. Phys.* **2002**, 116, 8973.
- (15) Baddeley, C. J. *Top. Catal.* **2003**, 25, 17.
- (16) Haq, S.; King, D. A. *J. Phys. Chem. B* **1996**, 100, 16957.
- (17) (a) Peng, Z.; Shlykov, S.; Van Alsenoy, C.; Geise, H. J.; Van der Veken, B. *J. Phys. Chem.* **1995**, 99, 10201. (b) Maes, I. I.; Herrebout, W. A.; Van der Veken, B. *J. Raman Spectrosc.* **1994**, 25, 679.
- (18) (a) Zahidi, E.; Castonguay, M.; McBreen, P. H. *Chem. Phys. Lett.* **1995**, 236, 122. (b) Wang, J.; Castonguay, M.; Roy, J.-R.; Zahidi, E.; McBreen, P. H. *J. Phys. Chem. B* **1999**, 103, 4382.
- (19) Syomin, D.; Koel, B. E. *Surf. Sci.* **2002**, 498, 53.
- (20) Lavoie, S.; Laliberte, M.-A.; McBreen, P. H. *J. Am. Chem. Soc.* **2003**, 125, 15756.
- (21) (a) Wilmshurst, J. K.; Horwood, J. F. *Aust. J. Chem.* **1971**, 24, 1183. (b) Dhan, V.; Gupta, R. K. *Indian J. Pure Appl. Phys.* **1996**, 34, 830. (c) Castonguay, M.; Roy, J.-R.; McBreen, P. *J. Am. Chem. Soc.* **2000**, 122, 518.
- (22) Laliberté, M.-A.; Lavoie, S.; McBreen, P. H. Manuscript in preparation.
- (23) Bonello, J. M.; Lambert, R. M.; Kunzle, N.; Baiker, A. *J. Am. Chem. Soc.* **2000**, 122, 9864.
- (24) (a) Rochefort, A.; McBreen, P. H. *J. Phys. Chem. A* **2001**, 105, 1320. (b) Burgi, T.; Atamny, F.; Schlögl, R.; Baiker, A. *J. Phys. Chem. B* **2000**, 104, 5943.
- (25) (a) Vaz, P. D.; Ribeiro-Claro, P. J. A. *J. Phys. Chem. A* **2003**, 107, 6301. (b) Vaz, P. D.; Ribeiro-Claro, P. J. A. *J. Raman Spectrosc.* **2003**, 34, 863.
- (26) Solcà, N.; Dopfer, O. *J. Phys. Chem. A* **2003**, 107, 4046.
- (27) Manojkumar, T. K.; Choi, H. S.; Hong, B. H.; Tarakeshwar, P.; Kim, K. S. *J. Chem. Phys.* **2004**, 121, 841.
- (28) Venkatsen, V.; Fujii, A.; Ebata, T.; Mikami, N. *Chem. Phys. Lett.* **2004**, 394, 45.
- (29) (a) Morin, C.; Simon, D.; Sautet, P. *J. Phys. Chem. B* **2004**, 108, 5643. (b) Mittendorfer, F.; Thorazeau, C.; Raybaud, P.; Toulhoat, H. *J. Phys. Chem. B* **2003**, 107, 12287.
- (30) Lavoie, S.; Laliberte, M.-A.; McBreen, P. H. *Catal. Lett.* **2004**, 97, 111.
- (31) Hutchings, G. J. *Ann. Rev. Mater. Res.* **2005**, 35, 43.
- (32) Burgi, T.; Baiker, A. *Acc. Chem. Res.* **2004**, 37, 909.
- (33) (a) LeBlanc, R. J.; Chu, W.; Williams, C. T. *J. Mol. Catal. A: Chem.* **2004**, 212, 277. (b) Calvo, S. R.; LeBlanc, R. J.; Williams, C. T.; Balbuena, P. B. *Surf. Sci.* **2004**, 563, 57. (c) Ferri, D.; Burgi, T. *J. Am. Chem. Soc.* **2001**, 123, 12974. (d) Kubota, J.; Zaera, F. *J. Am. Chem. Soc.* **2001**, 123, 12074. (e) von Arx, M.; Wahl, M.; Jung, T. A.; Baiker, A. *Phys. Chem. Chem. Phys.* **2005**, 7, 273.
- (34) Orglmeister, E.; Mallat, T.; Baiker, A. *Adv. Synth. Catal.* **2005**, 347, 78.
- (35) Yamamoto, H.; Futasugi, K. *Angew. Chem., Int. Ed.* **2005**, 44, 1924.
- (36) Evans, D. A.; Rovis, T.; Kozlowski, M. C.; Tedrow, J. S. *J. Am. Chem. Soc.* **1999**, 121, 1994.
- (37) (a) Pihko, P. M. *Angew. Chem., Int. Ed.* **2004**, 43, 2062. (b) Huang, Y.; Unni, A. K.; Thadani, A. N.; Rawal, U. H. *Nature* **2003**, 424, 146.
- (38) (a) Vargas, A.; Burgi, T.; Baiker, A. *J. Catal.* **2004**, 226, 69. (b) Burgi, T.; Baiker, A. *J. Catal.* **2000**, 194, 445.